

Project 1 Report

Se Hwan Jeon

January 30, 2020

1 Human Arm Model

A planar model of the human arm was developed from the structure of the vertical model used by Ogihara and Yamazaki, shown in Figure 1 [1]. As the position of the wrist was moved in a circular path, the joint angles, torques, and forces for the shoulder and elbow were calculated for each configuration. For the path followed, it was required that the shoulder and elbow angle would exceed a range of 45° . Two quantities were then optimized: the total force of the engaged muscles at each configuration, and the total activation of the muscles (defined as the force exerted by the muscle divided by its maximum) at each configuration.

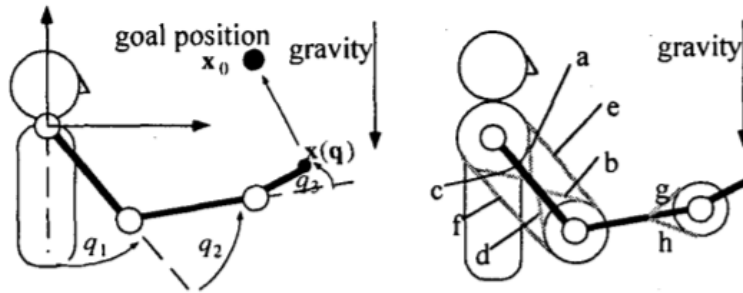


Figure 1: Vertical model of human arm complex. $a - h$ represent muscles acting on the links of the arm. The corresponding muscles for $a - h$ is detailed in Appendix A [1].

1.1 Assumptions

A number of assumptions were made to perform the analysis described.

- All motion is solely parallel to the vertical, sagittal plane.
 - The human arm consists of three rigid links consisting of the upper arm, forearm, and wrist.
-

- The analysis will not consider the flexion of the wrist, and the angle q_3 in Figure 1 will equal 0° for all configurations and the forces applied from g and h will be ignored.
- The moment arms of the engaged muscles were assumed to be constant for all configuration positions.
- Only the defined muscles $a - h$ in Figure 1 control the movement of the arm, and act as pure force generators.
- The path is independent of the required muscle forces.
- At each configuration along the path, there are no dynamics effects from velocity or acceleration.
- The length-tension and velocity-tension relationships for muscles will be ignored.
- There is no change in physiological cross-sectional area (PCSA) of the muscles.

2 Results

2.1 Motion Path Configuration

To determine the motion path of the arm complex, the radius and center of the circular path were defined as r_c and (x_c, y_c) respectively, as shown in Figure 2.

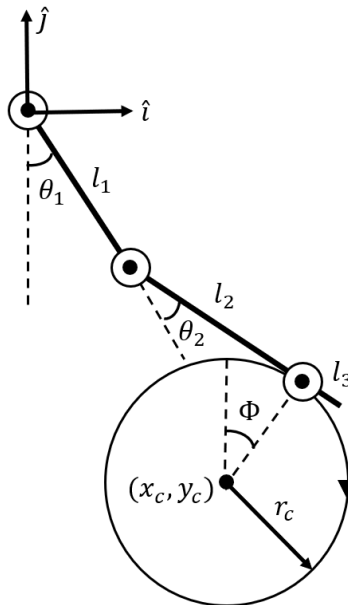


Figure 2: Developed model of human arm complex.

To ensure the path would not exceed the maximum length of the arm, the following condition was enforced

$$\sqrt{x_c^2 + y_c^2} + r_c \leq l_1 + l_2, \quad (1.1)$$

where l_1 and l_2 are the lengths of the upper arm and forearm respectively, and can be found in Appendix A [1]. An appropriate position and radius chosen for the analysis was $x_c = 0.15$ m, $y_c = -0.3$ m, and $r_c = 0.2$ m, but many other configurations would also be possible.

From the defined system, equations for the vertical and horizontal position of the wrist could be defined as a function of θ_1 , θ_2 , and ϕ , given below as

$$x_w = l_1 \sin(\theta_1) + l_2 \sin(\theta_1 + \theta_2) = x_c + r_c \sin(\phi), \quad (1.2)$$

$$y_w = -l_1 \cos(\theta_1) - l_2 \cos(\theta_1 + \theta_2) = y_c + r_c \cos(\phi), \quad (1.3)$$

where x_w and y_w are the horizontal and vertical position of the wrist with respect to the origin (the shoulder joint).

ϕ was varied from 0° to 360° with 1000 intermediate points, and the system of two equations was solved for the two unknowns, θ_1 and θ_2 for each ϕ using MATLAB's `solve` command. At each position, two unique solutions exist with the elbow in a "convex" or "concave" orientation. The analysis was performed with the elbow always in a "concave" position by giving an initial guess to the solver close to the desired orientation angles.

The resultant plots of θ_1 and θ_2 vs. ϕ show the evolution of the shoulder and elbow angles as a function of the wrist's position along its path, as shown in Figure 3.

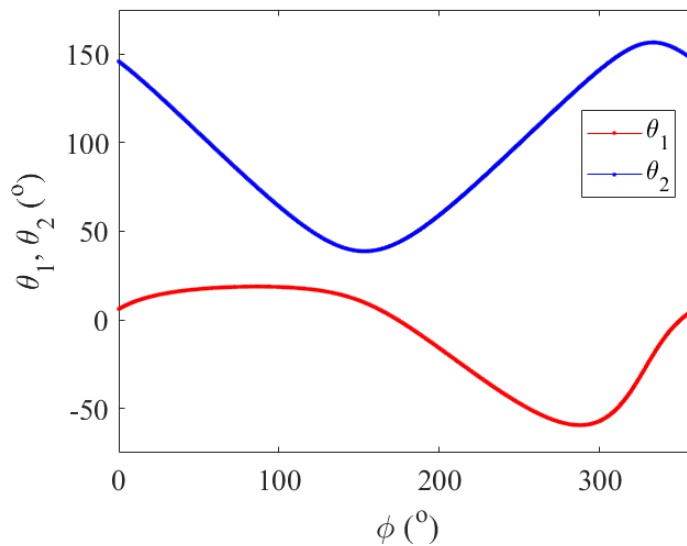


Figure 3: Plot of θ_1 and θ_2 vs. ϕ .

The range for θ_1 was 78.2° , and the range for θ_2 was 117.8° , satisfying the minimum range of 45° .

2.2 Joint Torques

At each position along the defined circular path, the joint torques necessary to statically hold the arm were calculated. Only the weight forces from the upper arm, forearm, and hand were considered, and the forearm and hand were considered one rigid link. Masses and proximal distances to the centers of mass for each segment are shown in Appendix A [1]. Free body diagrams were drawn for individual segments to determine the torque at the shoulder and elbow (τ_s and τ_e respectively) under static conditions, and the resulting equations were used to calculate the torques at each value of ϕ , shown in Figure 4.

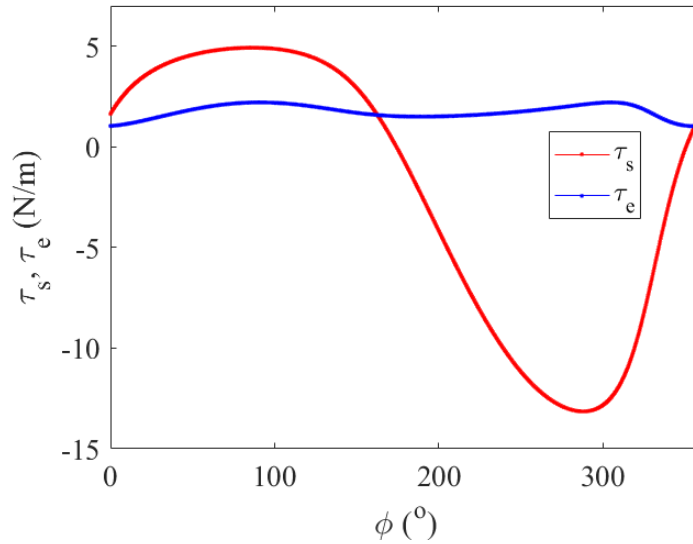


Figure 4: Plot of τ_s and τ_e vs. ϕ .

2.3 Muscle Force Analysis

To generate the torques required to hold the arm in quasi-equilibrium at each position, the muscles forces acting on each segment were multiplied by their respective moment arms and summed to equal the net torques on the shoulder and elbow. These moment arms are shown in Appendix A [1]. The torques in the shoulder and elbow can then be expressed as

$$\mathbf{T} = \mathbf{GF}, \quad (1.4)$$

where \mathbf{T} is the vector of torques for the shoulder and elbow, \mathbf{G} is a 2×6 matrix of moment arms and \mathbf{F} is the vector of muscle forces $a - f$.

2.4 Muscle Force Optimization

Two quantities were considered to be minimized in the defined system. The first was the total force exerted by the muscles in the arm, and the second was the total *activation* of the muscles in the arm, given below as

$$f_1(\mathbf{F}) = \sum_{i=a}^{i=f} F_i, \quad (1.5)$$

$$f_2(\mathbf{F}) = \sum_{i=a}^{i=f} \frac{F_i}{F_{i,max}}, \quad (1.6)$$

where f_1 and f_2 are the objective functions, F_i is the force of the muscle, and $F_{i,max}$ is the maximum force of that specific muscle, shown in Appendix A [1].

For the cases, the following constraints and bounds were defined.

$$\mathbf{F} \leq \mathbf{F}_{\max}, \quad (1.7)$$

$$\mathbf{T} = \mathbf{GF}, \quad (1.8)$$

$$\mathbf{F} \geq \mathbf{0}, \quad (1.9)$$

where \mathbf{F}_{\max} is a vector of the maximum forces for each of the muscles.

MATLAB's `fmincon` function was used with the above constraints to minimize the objective functions at each configuration of ϕ . The plots of the active muscle forces for the first and second optimization studies as a function of ϕ is shown below in Figure 5 and 6 respectively.

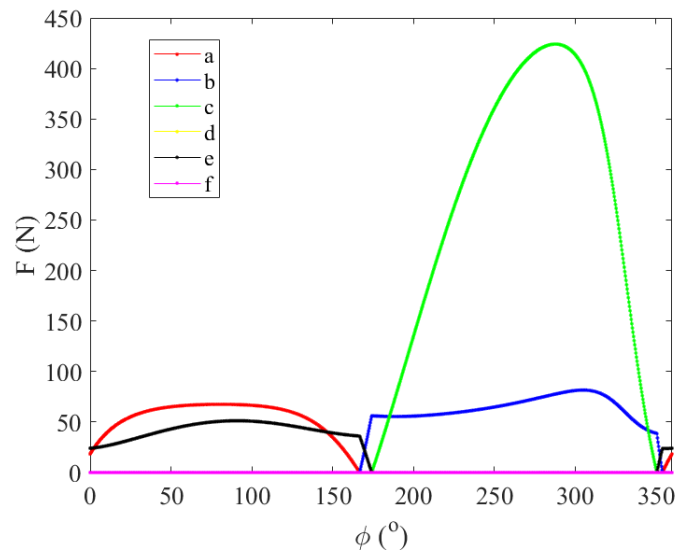


Figure 5: Plot of muscle forces vs. ϕ when total force is minimized.

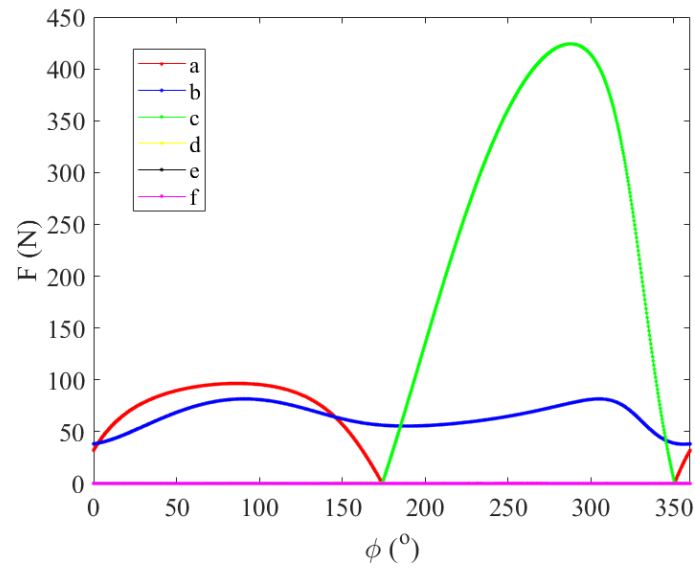


Figure 6: Plot of muscle forces vs. ϕ when total muscle activation is minimized.

The total force for both cases and the total activation for both cases was also plotted as a function of ϕ , as shown in Figure 7 and 8.

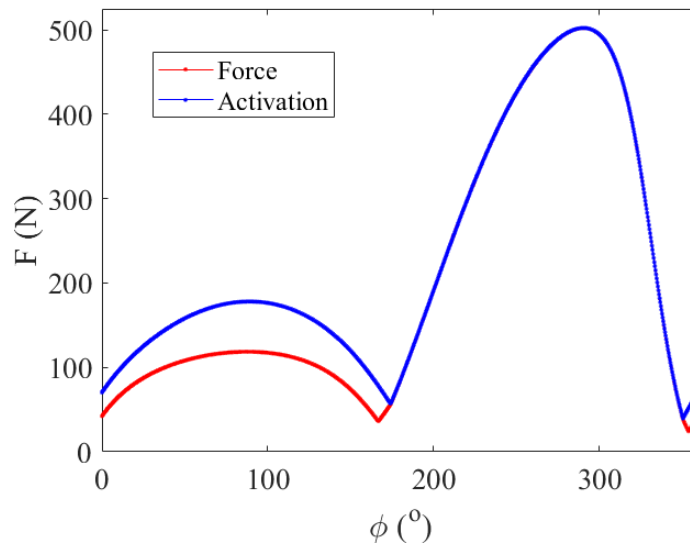


Figure 7: Plot of total force vs. ϕ for optimized force and optimized activation.

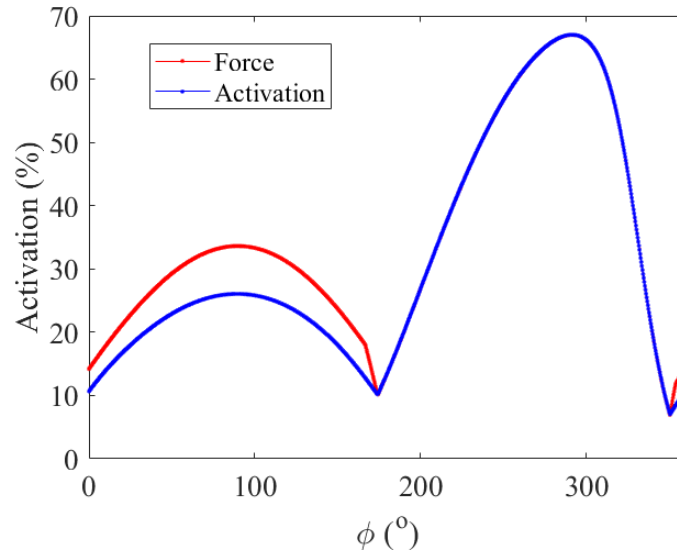


Figure 8: Plot of total activation vs. ϕ for optimized force and optimized activation. Note that the quantified activation is the sum of the activations of all six muscles, and its maximum value would be 600%, not 100%.

3 Discussion

For all values of ϕ , muscles d and f , the M. triceps brachii breve and M. triceps brachii longue are not needed to statically hold the arm in each position. This is most likely due to the prescribed motion of the arm, and if the radius or center was changed, these muscles may be used actively to hold the arm. Interestingly, when activation is optimized, muscle e , the M. biceps brachii, is also unused to sustain the weight of the arm.

The resulting torques were greatest at around $\phi = 290^\circ$, and muscle c , the M. latissimus dorsi, appears to be most responsible for moving the arm complex to that configuration regardless of which quantity is being optimized for.

From Figures 7 and 8, for ϕ between around 0° and 170° , optimizing for activation resulted in a total force expenditure of at least 50% greater than the total force being optimized. Similarly, optimizing for total force results in a roughly 10% maximum increase in total activation compared to the minimum possible values. When the arm is close to the body, it appears that there is little to no difference in optimizing for total force or activation, but as the arm is extended, there is more variability in which muscles are engaged and to what extent.

References

- [1] Ogihara, N., and Yamazaki, N., 1999, "Generation of human reaching movement using a recurrent neural network model," In Proceedings of IEEE International Conference on Systems, Man, and Cybernetics, 2, pp. 692697.

Appendix A: Muscle Parameters

	Max Force[N]	MA[m]	
a. M. pectoralis major	840	-0.051(s)	
b. M. brachialis	560	-0.027(e)	
c. M. latissimus dorsi	800	0.041(s)	
d. M. triceps brachii breve	480	0.020(e)	
e. M. biceps brachii	200	-0.029(s)	-0.043(e)
f. M. triceps brachii longue	240	0.025(s)	0.023(e)
g. M. flexor carpi rad & ulna	141	-0.017(w)	
h. M. ext carpi rad & ulna	144	0.019(w)	

Note: MA=moment arm, (s), (e) and (w) denote MA around shoulder, elbow, and wrist joints, respectively.

Figure 9: Muscle designations, forces, and moment arms [1].

	mass[kg]	length[m]	C.G[m]	Inertia[kgm ²]
Upper arm	1.68	0.320	0.141	0.0133
Fore arm	0.96	0.247	0.106	0.0067
Hand	0.36	0.184	0.094	0.0006

Figure 10: Inertial and geometric parameters of upper arm, forearm, and hand [1].